

pubs.acs.org/estengg Article

An Investigation of Thermal Air Degradation and Pyrolysis of Perand Polyfluoroalkyl Substances and Aqueous Film-Forming Foams in Soil

Ali Alinezhad, Pavankumar Challa Sasi, Ping Zhang, Bin Yao, Alena Kubátová, Svetlana A. Golovko, Mikhail Y. Golovko, and Feng Xiao*



Cite This: ACS EST Engg. 2022, 2, 198-209



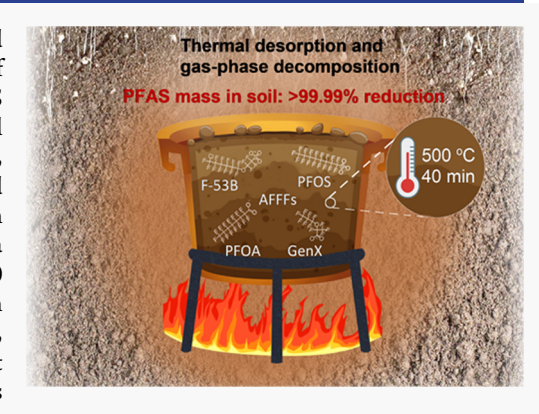
ACCESS I

III Metrics & More



s Supporting Information

ABSTRACT: In this study, we found that thermal decomposition of per- and polyfluoroalkyl substances (PFAS) in soil was rapid at moderate temperatures of $400-500\,^{\circ}\text{C}$, regardless of whether the soil was contaminated by a single PFAS compound or a PFAS mixture in aqueous film-forming foams. Substantial degradation (>99%) of PFAS in soil, including perfluorooctanoic acid (PFOA), perfluorooctane sulfonate (PFOS), short-chain homologues, cationic and zwitterionic precursors, and PFOA and PFOS alternatives, occurred in 30 min at 500 °C in both a sealed reactor in air and a horizontal reactor under a continuous flow of N₂. The effect of the initial PFAS level in soil (0.001–10 μ mol/g) and soil texture was insignificant, provided a sufficiently high temperature was applied. Furthermore, this study showed, for the first time, that kaolinite dramatically decreased the apparent yield of F from PFAS heated at >300 °C, likely due to the chemisorption of F radicals on kaolinite. This phenomenon was not observed when kaolinite and an inorganic fluoride salt



(NaF) were thermally treated. Lastly, various nonpolar thermal degradation products of PFOA and PFOS were reported for the first time. The profile of fluorinated volatiles, particularly perfluoroalkenes, was similar between these two chemicals. The results support a radical-mediated degradation pathway of PFAS.

KEYWORDS: soil remediation, AFFF, GenX, F-53B, radical-chain mechanism

■ INTRODUCTION

Per- and polyfluoroalkyl substances (PFAS) are synthetic organofluorine chemicals that have been mass-produced since the 1950s for a variety of high-temperature resistant products, such as nonstick cookware and aqueous film-forming foams (AFFFs) for firefighting devices. 1-3 More than 3000 PFAS might have been manufactured,⁴ and more than 750 PFAS have been identified in environmental and biological samples. 5-14 Long-chain PFAS bioaccumulate in food chains, 13,15-18 leading to ecological and human health risks. 19-22 Widespread PFAS occurrence in the environment has caused great concern among the scientific community, policymakers, and the general public. The USEPA plans to regulate two primary PFAS, perfluorooctanoic acid (PFOA) and perfluorooctanesulfonic acid (PFOS), under the Safe Drinking Water Act.²³ The global historical production of PFOA and related chemicals was estimated to be 3600-5700 t between 1951 and 2004.2 The estimated global production of PFOS and a major precursor compound (perfluorooctane sulfonyl fluoride) was 122,500 t between 1970 and 2002. Both PFOA and PFOS are resistant to degradation 24-27 and difficult to remove during conventional water and wastewater treatment.^{25,27–29} The revised EU Water Framework Directive, which is subject to the final approval by the EU parliament, proposes a limit value of 100 ng/L for a total of 20 PFAS, including PFOA, PFOS, and their short-chain homologues.³⁰ Certain short-chain PFAS are being included in the list of Persistent Mobile and Toxic substances.³¹

Perfluoroalkyl carboxylic acids (PFCAs, e.g., PFOA) and perfluoroalkyl sulfonic acids (PFSAs, e.g., PFOS) are non-volatile at ambient temperature, ionic or ionizable at circumneutral pH (6–9), moderately hydrophobic, and soluble in water. If released to the soil, they may interact with soil organic matter and sorb to soil particles, posing a threat to human health through both direct and indirect routes of exposure, including ingestion and inhalation of fugitive soil particles³² and PFAS transfer from soil to crops. ^{33,34} PFAS can

Received: September 15, 2021
Revised: December 22, 2021
Accepted: December 30, 2021
Published: January 11, 2022





also move off-site and reach drinking-water sources (surface water and groundwater) via runoff or leaching. 32,35-37 It was previously estimated that ingestion of contaminated groundwater constitutes a more important route of exposure to PFOA and PFOS than ingestion of contaminated soil.³² AFFF-impacted sites, ^{36,38,39} PFAS manufacturing facilities, ^{32,40–42} and landfills^{43,44} constitute predominant point sources of soil contamination of PFAS, whereas land application of PFAScontaining biosolids 45,46 and reclaimed wastewater 47 are nonpoint contamination sources in rural areas. More than 400 sites have been identified in the United States where known or suspected release of PFAS to soil has occurred due to the use of AFFFs for fire training.⁴⁸ PFOA and PFOS at levels up to 10,000 ng/g were observed in contaminated soil near point sources (see Figure 2 of ref 32). Remediation of PFAS-contaminated sites is currently a national priority in the United States.

A few treatment and remediation approaches have been investigated for removing PFAS from contaminated water and soil, including solvent flushing, ⁴⁹ photocatalytic degradation, ^{50–52} sequestration, ^{53,54} ball milling, ⁵⁵ electrochemical approaches, ^{56,57} and hydrothermal methods. ^{58,59} The remediation efficiency, however, may be strongly influenced by the concentration of PFAS in the treated media and the properties (e.g., functionality and chain length) of PFAS. PFAS are relatively difficult to remove from soil by conventional physical and chemical means. In an interim guidance, USEPA has identified thermal treatment as one of the technological solutions that is commercially available and has the capacity to degrade or manage the migration of PFAS in contaminated materials. ⁶⁰ Recent laboratory studies have reported that thermal treatment is highly effective for decontaminating PFAS-containing materials, including soil, ^{61,62} activated carbon, ^{63–65} and sludge. ⁶⁶

Thermal decomposition of PFAS molecules involves a series of physical transitions, such as melting and evaporation, and multistep chemical reactions, including radical-mediated initiation, chain propagation, recombination, chain stripping (for polyfluorinated compounds⁶⁷), and termination.⁶⁸ Our group recently reported that two types of initiations are likely involved: 64,65,67,68 end-chain scission and random-chain scission. Thermal decomposition of PFCAs, PFSAs, and polyfluorinated compounds yields various transient intermediates, including shorter-chained PFAS and underreported PFAS that are nonvolatile at room temperature. 64,67 Granular activated carbon (GAC), or other highly porous materials, can adsorb gas-phase PFCA molecules, alter thermal decomposition pathways, and substantially accelerate PFCA decomposition at low and moderate temperatures (<400 °C).64

Despite the insights gained from previous studies, a fundamental understanding in certain vital aspects of PFAS thermal decomposition is still limited and fragmented. Information on volatile, nonpolar thermal decomposition products of PFAS compounds is sparse in the literature. By means of gas-phase nuclear magnetic resonance (NMR), Krusic and Roe identified 1H-perfluoroheptane (C_7HF_{15}) and perfluoro-1-heptene (C_7F_{14}) as thermal decomposition products of PFOA. 69 However, because of the generally low sensitivity and selectivity of NMR, it is unclear whether these two species are the only nonpolar thermal decomposition products of PFOA. Information on nonpolar thermal decomposition products of other PFAS chemicals, such as

PFOS, is practically nonexistent in the literature. This information is critically needed because the environmental impact associated with these products can be significant. Based on our previous results, ^{64,65,67,68} we tested the hypothesis in this study that free-radical degradation of the perfluorinated chain of PFAS yields unsaturated perfluorocarbons (e.g., perfluoroalkenes).

Furthermore, a few key parameters that may affect the thermal remediation of PFAS-contaminated soils have been understudied or overlooked. A significant heating time of up to 14 days or a very high heating temperature, such as >1000 °C, was used previously in cleaning up soils contaminated with PFAS. Because the costs of remediation rise significantly with the treatment temperature and time, the effect of the temperature—time profile needs to be established. Likewise, the effect of the initial PFAS level in the soil and the soil texture need to be investigated.

Since the production of PFOS, PFOA, and related compounds was phased out, ^{70,71} alternatives (e.g., GenX and F-53B) have been produced and introduced in the market. ^{4,72} GenX is a relatively new PFOA alternative, ^{6,73,74} while F-53B has been manufactured for several decades as an alternative to PFOS. ^{7,8} In GenX and F-53B, perfluoroalkyl segments are connected by ether linkage(s). Both chemicals have been detected in the surface soil at concentrations of 100 ng/g. ^{75,76} The thermal stability and degradation behaviors of fluorinated ether compounds have remained elusive. This study was carried out to delineate these factors that impact the fate of PFAS in soil during heating and influence the selection and operation of thermal technologies for the remediation of PFAS-contaminated sites.

■ MATERIALS AND METHODS

PFAS Chemicals. The present study included 18 PFAS chemicals in six classes (Table S1 in the Supporting Information) as well as two AFFF samples that contain a mixture of PFAS (Table S2).⁶⁷ These 18 PFAS included seven legacy PFCAs and PFSAs, two legacy anionic PFAS, and PFOA and PFOS alternatives: perfluorobutyric acid (PFBA), perfluoropentanoic acid (PFPeA), perfluoroheptanoic acid (PFHpA), PFOA, perfluorononanoic acid (PFNA), perfluorodecanoic acid (PFDA), perfluoroundecanoic acid (PFUn-DA), and potassium salts of perfluorobutanesulfonic acid (PFBS), perfluorohexanesulfonic acid (PFHxS), PFOS, hexafluoropropylene oxide dimer acid (HFPO-DA), 6:2 chlorinated polyfluorinated ether sulfonate potassium salt (6:2 Cl-PFAES; the major component of F-53B), 2-(Nmethylperfluorooctanesulfonamido)acetic acid (N-MeFO-SAA), and the sodium salt of 8:2 fluorotelomer sulfonate (8:2 FTS). Furthermore, the test set also included four cationic and zwitterionic PFAS, perfluorooctaneamido ammonium salt (PFOAAmS, C₁₄H₁₆F₁₅N₂OI), perfluorooctanesulfonamido ammonium salt (PFOSAmS, C₁₄H₁₆F₁₇N₂O₂SI), perfluorooctaneamido betaine (PFOAB, $C_{15}H_{16}F_{15}N_2O_3$), and perfluorooctanesulfonamido betaine (PFOSB, C₁₅H₁₆F₁₇N₂O₄S) (Table S1). These cationic and zwitterionic substances have been detected in AFFFs and Fluorad brand surfactant samples^{5,10,11} and can be degraded to PFOA and PFOS in chemical,⁷⁷ biological,⁷⁸ and thermal⁶⁷ processes. Cationic and zwitterionic PFAS account for approximately 50% of newly identified PFAS compounds³ and have been found to compose up to 97% of the total PFAS mass in soils of a fire-training area.⁷⁹

We considered two scenarios (#1 and #2) in our experiments to illustrate the effect of five factors (Figure S1): two thermal parameters (heating temperature and heating time), PFAS properties, soil texture, and PFAS concentration in soil.

Soils. The heating experiments in both scenarios were conducted using a natural soil that is a clay loam with a soil organic matter of 9.8% and a reference kaolinite clay (KGa-1b; Clay Minerals Society). Ottawa sand (Fisher Scientific) and Pahokee peat (IHSS, St. Paul, MN) were included in certain experiments to examine the effect of soil texture. Soil samples were air-dried before use in thermal treatment experiments.

Scenario #1: Adsorption and Thermal Decomposition of PFAS in Soil (Clay Loam and Kaolinite Clay). The preadsorption of PFAS chemicals in soil was performed in batch sorption experiments following the procedure described previously (or see the Supporting Information).80 The liquid phase was a landfill leachate sample provided by Waste Management Inc. No measurable PFAS (n = 18; Table S1) were detected in microfiltered landfill leachate samples. To facilitate detection, the leachate samples were spiked with PFAS to $\sim 2 \times 10^{-6}$ mol/L in the laboratory. The apparent sorption equilibrium was reached after 2 days. After sorption, the supernatant fluid was decanted. The sorption equilibrium concentration of PFOA ranged up to ~0.9 µmol/L that is in the same order of magnitude for PFOA groundwater concentration in contamination hotspots.³² The remaining PFAS-laden soil particles were freeze-dried, stored in a desiccator to reach room temperature, and thermally treated in a sealed container using the procedure 64,65 described in the Supporting Information. Without specification, thermal decomposition experiments were performed in a sealed container in an air atmosphere.

The sorption data were fit to the Freundlich model

$$C_{\rm s} = K_{\rm F}(C_{\rm w})^n \tag{1}$$

where n is the Freundlich exponent providing an indication of isotherm nonlinearity and $K_{\rm F}$ [$(\mu {\rm mol/kg})(\mu {\rm mol/L})^{-n}$] is the Freundlich sorption coefficient. The parameters were obtained by a nonlinear least-squares regression weighted by the dependent variable. The observed distribution ratio ($K_{\rm d}$, $L/k_{\rm g}$) is defined as the adsorbed-to-solution concentration ratio

$$K_{\rm d} = C_{\rm s}/C_{\rm w} \tag{2}$$

 $K_{\rm d}$ is related to $K_{\rm F}$ by

$$K_{\rm d} = K_{\rm F} (C_{\rm w})^{n-1} \tag{3}$$

Soil particles laden with PFAS were split into two portions. One portion of the particles (e.g., 0.1 g) was extracted using methanol ($V_{\rm extr}$, 25 mL) containing ammonium acetate at 100 mol/L, ⁶⁵ and the mixture was sonicated for 30 min. The PFAS mass before thermal treatment ($M_{\rm PFAS,solid,initial}$) was computed using eq 4

$$M_{\rm PFAS, solid, initial} = (C_{\rm extr} \times V_{\rm extr})/E$$
 (4)

where E (%) is the extraction efficiency and $C_{\rm extr}$ (μ mol) is the concentration of PFAS in the extract measured using a Waters Acuity ultrahigh-pressure liquid chromatograph coupled with a Waters quadrupole time-of-flight mass spectrometer (Synapt G2-S, Waters Corporation, Milford, MA, USA). Analytical details are described in the Supporting Information. Our

extraction method achieved recoveries of 90.2-104.2% for PFAS from soil (Figure S2). The other portion of the PFASladen solid particles was placed in a precleaned, closed borosilicate glass container and heated in an air atmosphere within a muffle furnace (Neytech, Vulcan 3-550, USA) at a preset temperature (125, 150, 200, 300, 400, 425, 450, 475, and 500 °C) for a certain residence time. Furthermore, depending on the operating temperature, the residence time of thermal remediation can vary from a few minutes to hours or days.83 To understand the effect of treatment time, PFAS-laden solid particles were heated at a given temperature for different durations (7, 15, 22, and 40 min). After heat treatment and cool down, distilled water (DW) was added to the container to measure water-extractable fluoride ions (F⁻) or methanol containing 100 mmol/L ammonium acetate to measure residual PFAS (see the Supporting Information and Figure S2).65

Scenario #2: Thermal Decomposition of PFAS Loosely Associated with Soil. For the second scenario, experiments were performed by directly mixing PFAS chemicals or AFFF with soil particles to represent the free state of PFAS molecules in soil or those molecules weakly associated with soil particles (see the Supporting Information).

To understand the effect of atmosphere, pyrolysis of PFAS with kaolinite was conducted in a temperature-programmable two-zone quartz tube furnace (MTI Corporation, CA) under a flow of N_2 (200 mL/min). The mixture was heated at a rate of 10 °C/min to the desired final heat treatment temperature and held for 30 min. Off-gas from the furnace and residual PFAS chemicals in the off-gas were treated and analyzed in the same manner as described previously. 65

To examine the adsorption of F⁻ on kaolinite, an inorganic salt (NaF) was heated together with kaolinite at different temperatures. After heat treatment and cool down, DW was added to the container to measure water-extractable F⁻.

X-ray Diffraction and Fourier Transform Infrared. Kaolinite particles collected from PFAS thermal degradation experiments were stored in a desiccator for 2 days and characterized by X-ray diffraction (XRD) (SmartLab, Rigaku, Japan) and Fourier transform infrared (FTIR) spectroscopy using a Nicolet iSS spectrometer with an iDS ATR accessory (Thermo Scientific, Madison, WI, USA). XRD has been previously used to identify minerals formed between calcium compounds and F released from PFAS during thermal treatments.

Identification of Volatile Decomposition Products. Our team has put significant effort into identifying volatile thermal decomposition products of PFAS. Capturing all traceamount volatile decomposition products and analyzing them using conventional gas chromatography-mass spectrometry (GC-MS) were found not to be trivial tasks. In the present study, we employed thermal desorption—pyrolysis (TD—Pyr) (Frontier 3030D, Frontier Labs Inc., Japan) connected to a cryogenic trapping-GC-MS system (Agilent GC 7890 and 5975C MS; Santa Clara, CA) to detect the pyrolysis decomposition products of PFOA and PFOS. Analytical details can be found in the Supporting Information. TD-Pyr-GC-MS was used in our previous studies. 64,65 The newly included cryo-trap (CT) on the inlet of the GC column allows gaseous products to be cooled cryogenically and concentrated in the CT before GC-MS analysis, which may improve the sensitivity of detection. Because of the direct introduction of a sample, the TD-Pyr-CT-GC-MS system can capture

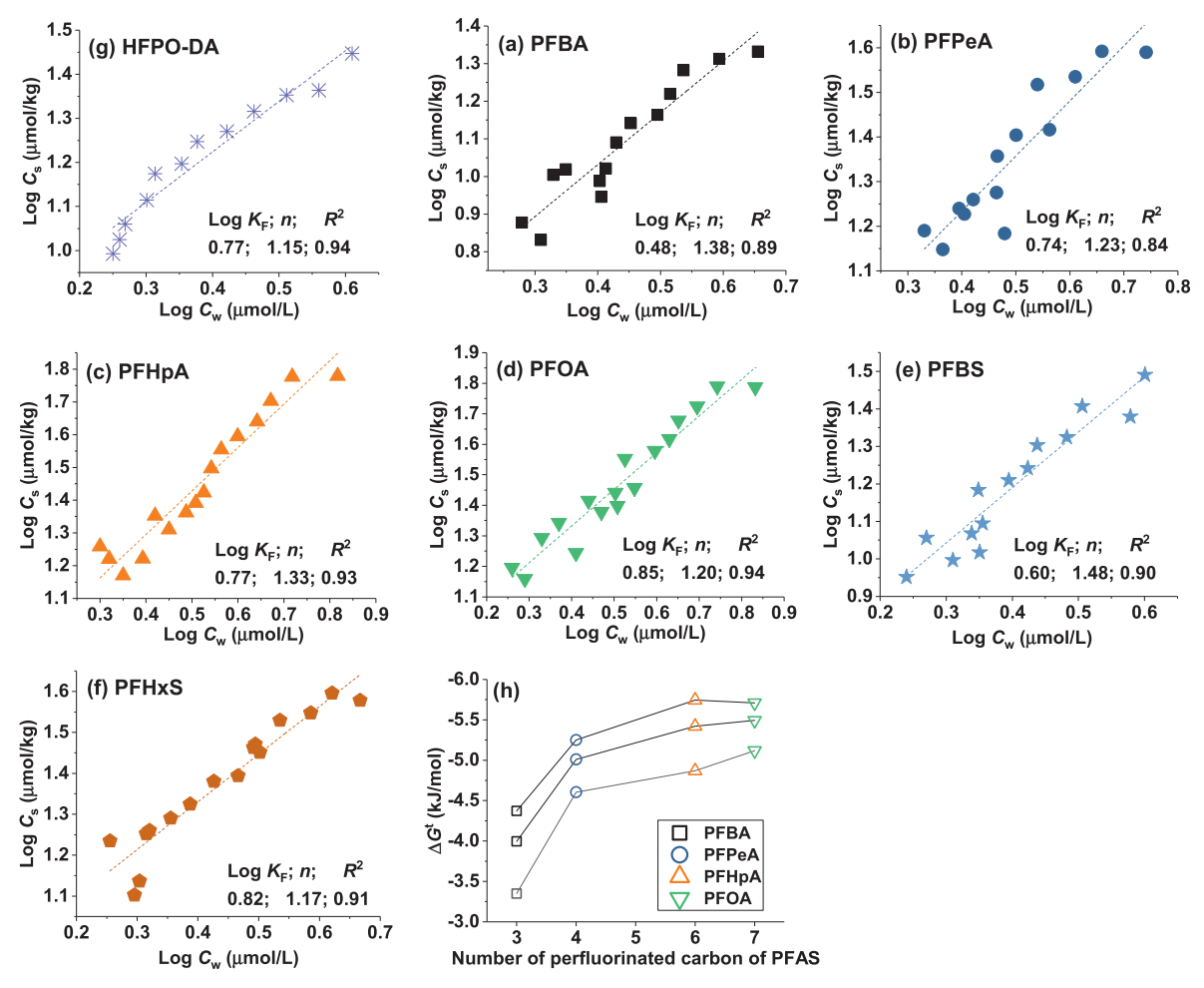


Figure 1. (a–g) Distribution of PFCAs, PFSAs, and HFPO-DA between kaolinite and landfill leachate. Dashed lines represent the fitting of adsorption data by the Freundlich model (eq 1). The Freundlich parameters (log $K_{\rm F}$; n) and the coefficient of determination (R^2) are also provided. (h) Free energy of adsorption ($\Delta G^{\rm t}$) as a function of the number of perfluorinated carbons in PFCAs. The $K_{\rm d}$ in the $\Delta G^{\rm t}$ calculation was computed at 2, 4, and 6 μ mol/L using eq 3 [three lines in (h)].

products/species that may not be detected by traditional GC–MS. Compounds were considered correctly detected when their GC–MS spectra presented a library match quality of \geq 80% or tentatively detected with a library match quality of 70–80%.

RESULTS AND DISCUSSION

PFAS Adsorption on Kaolinite from Landfill Leachate.

Soil and sediment sorption of anionic PFCAs and PFSAs has been investigated extensively and reviewed in detail. 84,85 The sorption of anionic PFAS species increases with the organic content of sediments, 84 the ionic strength of the solution, 81,86 and the perfluorinated carbon chain length. 81,84 Sorption isotherms of PFAS to soil/kaolinite/sediments from natural waters were generally either linear or nonlinear with a concavedownward curvature. 80,81,84,87–90

Figure 1 illustrates the adsorption of HFPO-DA and short-chain and long-chain PFCAs and PFSAs on kaolinite in landfill leachate. The isotherms display concave-upward curvatures, giving a Freundlich coefficient (n) of 1.15-1.45. This implies a decrease in adsorption as the concentration falls during the natural dilution of the liquid phase. Sorption of surfactants is typically characterized by a normal isotherm at a low concentration (region 1) and then a concave-upward curve due to the formation of hemimicelles (region 2) or micelles

(region 3).^{91–95} Landfill leachate is rich in dissolved organic matter that may reduce the critical micelle concentration of PFAS.⁹⁶ The concave-upward isotherms (Figure 1) may reflect the transition from region 1 to region 2.

The free energy of adsorption ($\Delta G^{\rm t}$) can be partitioned into terms representing the hydrophobic effect ($\Delta G^{\rm h}$), the electrostatic repulsion between PFAS anions and the negatively charged kaolinite surface ($\Delta G^{\rm e}$), and a lumped term ($\Delta G^{\rm o}$) for all other interactions, including dipolar, quadrupolar, and steric hindrance

$$\Delta G^{t} = \Delta G^{h} + \Delta G^{e} + \Delta G^{o} \tag{5}$$

Inherent in eq 5 is the assumption that weak attractive forces, such as dispersion, dipole—dipole, and quadrupole—quadrupole interactions, do not interfere with electrostatic interactions. The hydrophobic effect of PFAS originates from the disruption of the cohesive energy of water by the perfluoroalkyl chain, which drives PFAS molecules to the kaolinite surface. Although there is no unambiguous way to quantify the hydrophobic effect, the contribution of the fluorinated moiety (CF₂) to $\Delta G^{\rm h}$ can be expressed as ^{81,84,97}

$$\Delta G^{\rm h} = m \times \Delta G_{\rm CF_2} + b \tag{6}$$

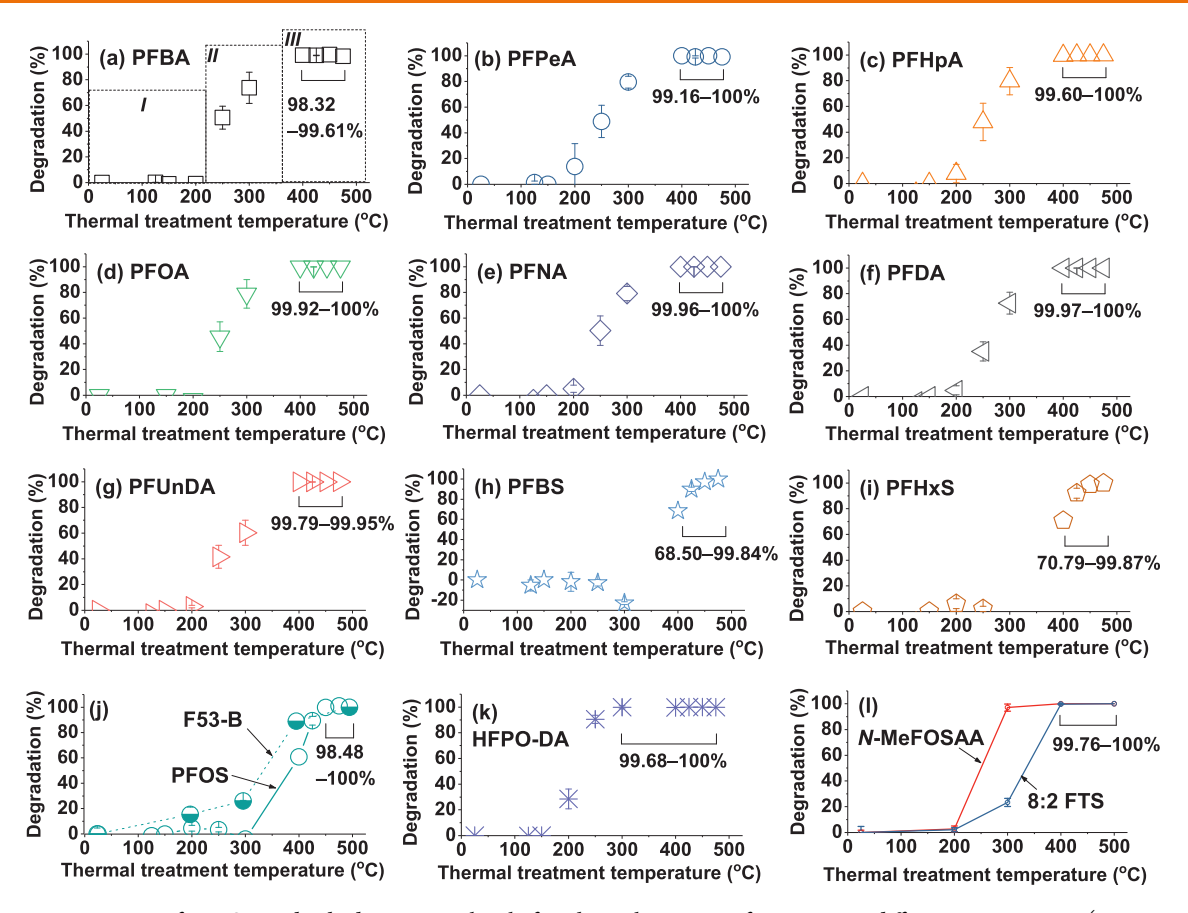


Figure 2. Decomposition of PFAS preadsorbed in a natural soil after thermal treatment for 30 min at different temperatures (scenario 1). Initial PFAS loading on soil (μ mol/ g_{soil}): PFBA, 0.0022; PFPeA, 0.0040; PFHpA, 0.0062; PFOA, 0.0097; PFNA, 0.019; PFDA, 0.047; PFUnDA, 0.079; PFBS, 0.0025; PFHxS, 0.0042; PFOS, 0.021; HFPO-DA: 0.0029; N-MeFOSAA: 0.030; 8:2 FTS: 0.026. The decomposition efficiency was assigned 100% if no measurable PFAS was found in soil after thermal treatment. The experiments (Figure 2) were performed in a sealed container in air. See Figure S3 for results obtained with a tube furnace under a flow of an inert gas (N_2).

where ΔG_{CF_2} is the hydrophobic contribution made by each CF₂ moiety driving PFAS to the kaolinite surface, m is the number of perfluorinated carbons in PFAS, and b is a constant. It was previously estimated that each CF₂ moiety contributed 2.5–2.7 kJ/mol to ΔG^{h81} or 0.5–0.6 log units to the measured distribution coefficients. ⁸⁴ By combining eqs 5 and 6, we can solve for ΔG^{t} in terms of m

$$\Delta G^{t} = m \times \Delta G_{CF_2} + \Delta G^{e} + \Delta G^{o} + b \tag{7}$$

Assuming ΔG^{e} and ΔG^{o} are independent of m, we can write

$$\Delta G^{\rm t} \propto m$$
 (8)

Consistent with eq 8, the value of $(-\Delta G^t)$ follows the order, PFBA < PFPeA < PFHpA \leq PFOA (Figure 1h), the same order as in the number of perfluorinated carbons, suggesting that the hydrophobic effect is a major driving force.

Thermal Decomposition of PFAS in Soil at Different Temperatures. Figures 2, S3–S6 illustrate the effect of temperature on PFAS decomposition in soil when heated for 30 min in air or N₂ (pyrolysis). Thermal decomposition or degradation in this study is defined as an irreversible process resulting in PFAS structure change, whereas thermal transformation refers to the formation of other species from a parent PFAS compound. As illustrated in Figures 2 and S3, the thermal decomposition efficiency of the studied PFAS in soil in the sealed (air) system was similar to that measured in a constant-pressure system under a flow of N₂, which is

consistent with our previous observations.^{64,65} However, future studies are needed to understand the effect of oxygen on thermal decomposition products and pathways of PFAS.

Three temperature regions were observed (I, II, and III): PFCAs in soil remained mostly stable at <200 °C, started to decompose at 200-400 °C, and decomposed almost completely in 30 min at ≥ 400 °C (Figures 2 and S3). PFSAs, on the other hand, are more thermally stable than PFCAs; a 30 min thermal treatment at 400 °C resulted in 60-71% degradation of PFSAs in the soil (Figures 2 and S3).

The decomposition of PFAS is related to the bond dissociation energies and other heteroatoms in the perfluorinated chain. Polyfluorinated compounds (*N*-MeFOSAA, 8:2 FTS, PFOAB, PFOAAmS, PFOSB, and PFOSAmS) and those present in AFFF samples exhibited near-complete degradation (>99%) in the soil when the temperature was ≥400 °C (Figures 2, S4, and S5). Because the nonfluorinated moiety is subject to side-chain stripping,⁶⁷ Polyfluorinated compounds are less thermally stable than perfluoroalkyl counterparts (e.g., PFOS; Figure 2).

The minimum temperature leading to decomposition (>30%) of PFOA and PFOS alternatives was 200 °C (Figure 2). Polyfluorinated ether sulfonate (6:2 Cl-PFAES; the major component of F-53B) appears to be more thermally stable than the perfluorinated ether carboxylic acid (HFPO-DA, i.e., the conjugate acid of GenX). Within 30 min, 99.8% of HFPO-DA and 26.0% of 6:2 Cl-PFAES decomposed at 300 °C. Both the

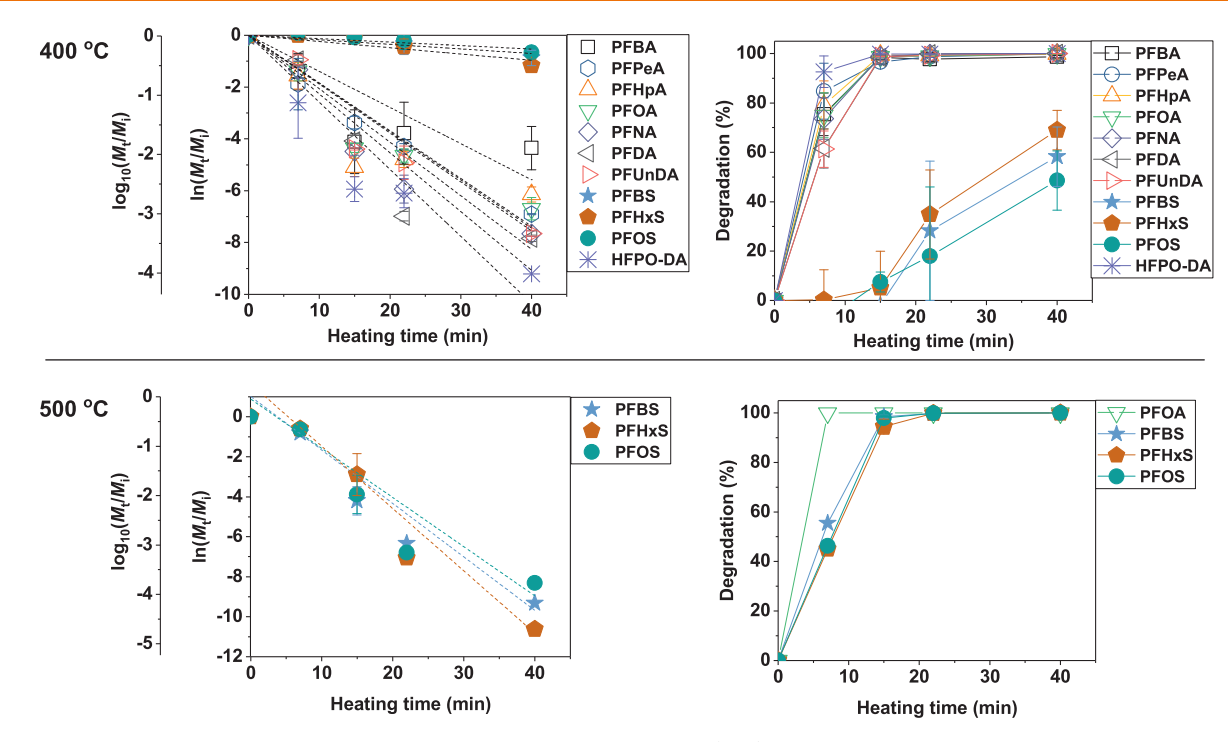


Figure 3. Thermal decomposition of PFAS in soil as a function of heating time (min) in a closed system with air. Initial PFAS loading on soil (μ mol/g_{soil}): PFBA, 0.0022; PFPeA, 0.0040; PFHPA, 0.0062; PFOA, 0.0097; PFNA, 0.019; PFDA, 0.047; PFUnDA, 0.079; PFBS, 0.0025; PFHXS, 0.0042; PFOS, 0.021; HFPO-DA: 0.0029. The dashed lines represent the best fit to the decomposition data using the first-order kinetic model.

fluorinated ether compounds (HFPO-DA and 6:2 Cl-PFAES) were more readily degraded by heating than the perfluoroalkyl counterparts (e.g., PFBA and PFOS) (Figure 2), which appears to be related to the ether group in the perfluorinated chain. Xiao et al. believed that PFAS thermal decomposition can occur through a random-chain scission pathway: the breaking off a C-C bond at seemingly random locations on the perfluorinated chain. From Bentel et al. calculated the bond dissociation energies of perfluoroalkyl ether carboxylic acids (PFECAs). The authors believed that the ether C-O bond in PFECAs (e.g., HFPO-DA) was prone to cleavage. The ether group in the perfluorinated chain of HFPO-DA and 6:2 Cl-PFAES may serve as a vulnerable bond scission site during thermal treatment.

Thermal Decomposition Kinetics. All curves of the residual mass of PFAS in soil versus the thermal treatment time were exponential in nature (Figure 3). At 400 °C, a considerable reduction (92.6%) in the total mass of HFPO-DA was observed following treatment for the shortest time used (7 min); however, the longer treatment time (15 min) resulted in an even larger reduction (99.7%). The PFCA mass also dropped dramatically in the first 7 min and continued to fall at an apparently slower rate for the next 30 min. The mass loss followed first-order kinetics. The apparent thermal decomposition half-lives ($t_{1/2, \rm thermal}$) of HFPO-DA, PFCAs, and PFSAs in soil at 400 °C were 2.7, 3.1–5.0, and 28.7–51.8 min, respectively. The decomposition of PFSAs (e.g., PFOS) occurred at a much slower rate at 400 °C (Figure 3).

At 500 °C, 99.99% degradation of PFOA was observed after heating for only 7 min (Figure 3). Thermal decomposition of PFSAs in soil was also significantly enhanced with a rise in temperature from 400 to 500 °C (Figure 3). A brief treatment for 7 min at 500 °C resulted in 45–55% degradation of all PFSAs in soil, while a treatment time of 15 min increased the extent of degradation to 94–98%. After 40 min, up to

99.9976% PFSAs, including PFOS, were degraded at 500 °C (Figure 3). A small portion of PFSAs, however, continued to decompose at a much slower rate. A longer treatment time or a higher decomposition temperature would be required to decontaminate the soil beyond a decontamination level of 99.9976% (Figure 3). The apparent thermal decomposition half-lives of PFSAs in soil were determined to be 2.4–3.1 min at 500 °C.

Effect of Initial PFAS Loading in Soil. The concentration of PFOA and PFOS in the soil can vary by 4 orders of magnitude, up to >10,000 ng/g $_{soil}$ in contamination "hotspots." At 400 °C, a consistently high decomposition rate (>98%) of PFCAs and HFPO-DA was observed over 4 orders of magnitude in concentration ranging from 0.00077 to \sim 24.2 μ mol_{PFCA}/g_{clay} (Figure 4). Heating at 400 °C was insufficient to degrade PFSAs in 30 min (Figure 3); therefore, an increase in PFSA loading led to an apparent decline in the thermal decomposition rate (Figure 4). The effect of initial loading became insignificant for PFSAs at 500 °C (Figure 4) at which they decomposed effectively (Figures 2 and 3). The residual PFSA mass dropped to <0.6% of the initial mass within 30 min at 500 °C, regardless of the initial level of PFSAs (Figure 4). Additionally, the effect of soil texture on thermal PFOA decomposition was found to be insignificant (Figure S6).

Apparent Yield of F. The quantification of F⁻ ions in water has been frequently performed using ion chromatography (IC). However, the measurement of F⁻ by IC can be hampered by the overlap of peaks of F⁻ and other anions, such as formate and acetate. In the present study, water-extractable F⁻ ions were quantified by (1) the USEPA SPADNS method used in our previous studies and (2) a F ion selective electrode (F-ISE). Both the methods yielded reliable results over a wide concentration range of F⁻ (Figure 5e,f). However, the detection limit of the SPADNS

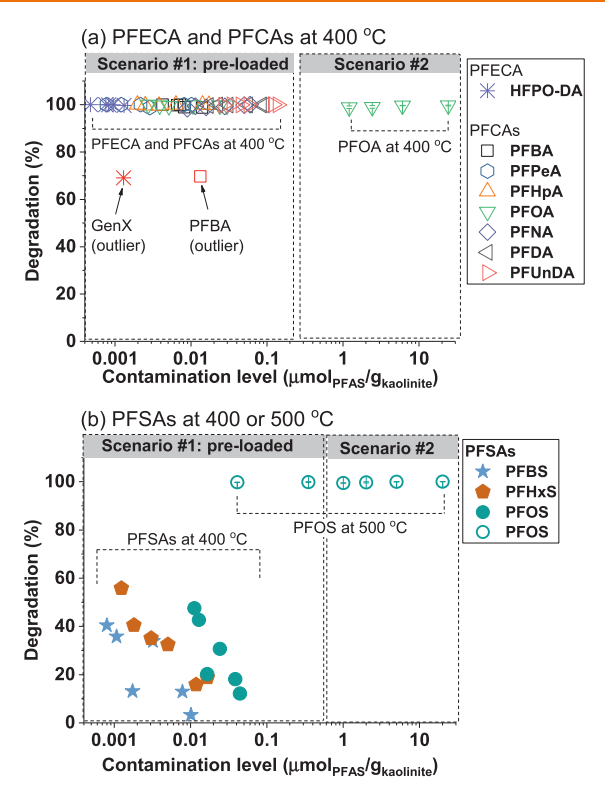


Figure 4. PFAS decomposition in kaolinite heated for 30 min at 400 and 500 $^{\circ}\text{C}$ as a function of initial loadings covering 4 orders of magnitude.

method is only 2 mg F⁻/L; a substantial dilution of a sample may cause dilution errors (Figure 5e).

Our team previously observed that the yield of F from both PFOA and PFOS increases with thermal treatment temperature, reaching >80 mol % at 700-900 °C.65 The presence of GAC can significantly enhance PFOA thermal decomposition at low and moderate temperatures (<400 °C) and increase the yield of F correspondingly.⁶⁴ In this study, the apparent yield of F from PFOA sharply declined with the presence of kaolinite (Figure 5), although the degradation of PFOA was not significantly affected (Figure S6). Similar results were also observed when PFOA was heated together with a natural soil (Figure S7). The measurable yield of F declined from 25.1 to 1.1 mol % when PFOA was heated at 400 °C with kaolinite at a mass ratio of 0.2 $g_{kaolinite}/\mu mol_{PFOA}$ (Figure 5a). The effect of kaolinite on the apparent yield of F from PFOA was significant only when the heating temperature was greater than 300 °C (Figure 5a), which became more pronounced with a rise in the mass ratio of kaolinite to PFOA (Figure 5b) and the heating time (Figure 5c).

Note that F⁻ ions were measured in the DW extract of PFOA and kaolinite after the thermal treatment. However, it is unlikely that the adsorption of F⁻ on kaolinite in DW caused the observed decline in F yield (Figure 5a-c) because no significant loss of F⁻ was found when NaF was heated with kaolinite and extracted with DW (Figure 5d). We postulate that the disappearance of measurable F illustrated in Figure 5a-c may have been caused by the reaction between kaolinite particles and F radicals^{64,65,67} generated during PFOA thermal

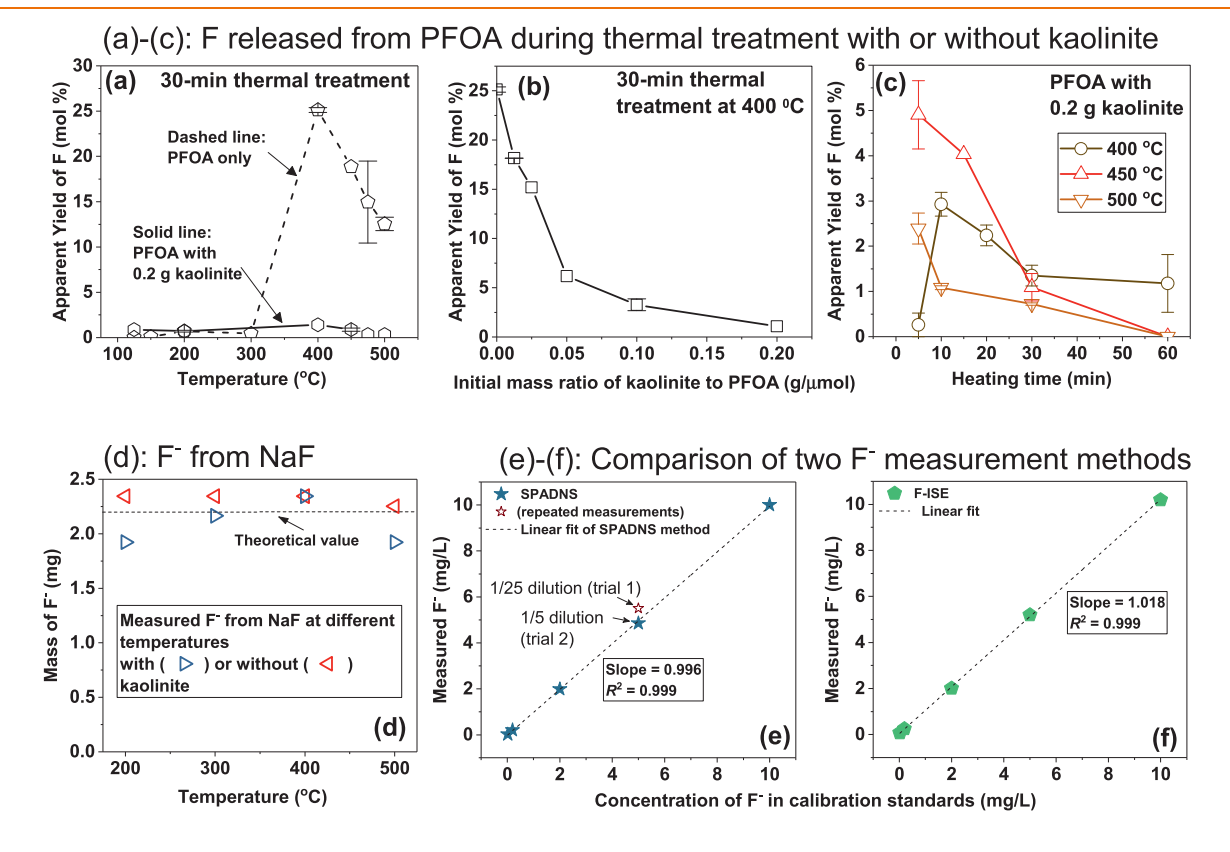


Figure 5. Apparent yield of F from PFOA during thermal treatment (initial mass: $1 \mu mol$) (a) as a function of the temperature with or without the presence of kaolinite (0.2 g), (b) as a function of the initial mass ratio of kaolinite to PFOA, and (c) as a function of the heating time at three temperatures. The F⁻ concentrations in the water extract were measured using the USEPA SPADNS method. (d) Measured mass of F⁻ after heating NaF (5 mg or 0.12 mmol) at different temperatures with or without the presence of kaolinite (0.2 g). The F⁻ concentrations in the water extract were measured with F-ISE. (e,f) Comparison of the two methods (SPADNS and F-ISE).

treatment. Such a reaction may not necessarily lead to the formation of new crystals such as cryolite $(Na_3AlF_6)^{101}$ because XRD and FTIR spectra did not exhibit peaks for new crystal phases or functional groups apart from the structure of kaolinite (Figures S8 and S9). However, it is also likely that XRD and FTIR are not sensitive enough to detect the newly formed crystalline phases. The thermal interaction mechanisms between F radicals and kaolinite are worthy of further study but are outside the scope of this paper.

Volatiles Generated from PFOA and PFOS upon Heating. Despite the difference in their structures, PFOA and PFOS generated a similar profile of fluorinated pyrolysis products (Figures 6 and S11–S18 and Table S3), including

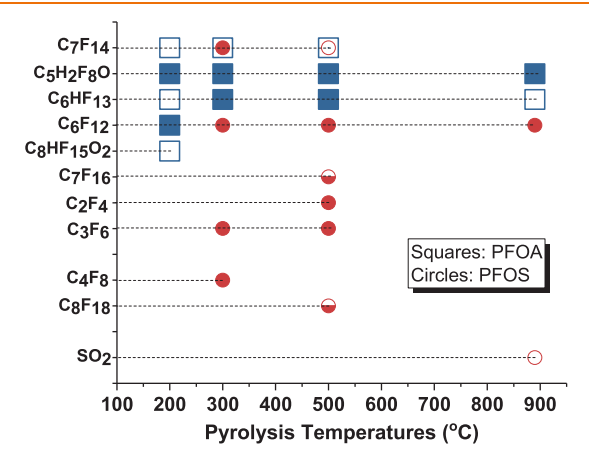


Figure 6. Detection of pyrolysis products of PFOA and PFOS by TD−Pyr−CT-GC−MS. Open symbols: library match quality of \geq 80%; half-filled symbols: library match quality of 70−80%; solid symbols: library match quality of \leq 70%.

unsaturated perfluorocarbons. This is consistent with our hypothesis. Perfluoro-1-heptene (C_7F_{14}) was identified as a thermal treatment product of PFOA and PFOS at 500 °C. Two C6 species, 1H-perfluorohexane (C₆HF₁₃) and perfluoro-1-hexene (C₆F₁₂), were also frequently detected. Short-chain perfluoroalkenes, including perfluoro-1-butene (C₄F₈), hexafluoropropene (C_3F_6) , and tetrafluoroethylene (C_2F_4) , were likely generated, but their MS library match qualities were less than 70%. The detection of perfluoroalkenes agrees well with the chain scission mechanism (Figure S10): the perfluoroalkyl chain is broken up from the bond between the perfluoroalkyl chain and the nonfluorinated moiety or at seemingly random locations on the perfluoroalkyl chain. This process forms perfluoroalkyl biradicals^{64,65} that successively relax to give perfluoroalkenes (Figure S10). Furthermore, pyrolysis of PFOS yielded long-chain perfluoroalkanes, including perfluorooctane (C_8F_{18}) and perfluoroheptane (C_7F_{16}) , following a chain-scission and recommendation mechanism (Figure S10).64,67 Previous researchers postulated that short-chain perfluoroalkanes, perfluoromethane (CF₄, m/z 88.0), and perfluoroethane (C₂F₆, m/z 138.0) are generated during the thermal treatment of PFOS; 102 however, no mass spectral evidence and literature data are available to support their hypothesis. In the current study, short-chain perfluoroalkanes were not detected.

Another interesting observation is that fewer volatile products were generated when PFAS was heated at 890 $^{\circ}$ C (Figure 6). Khan et al. calculated the theoretical thermal decomposition half-life of PFOS to be only 1 s at 727 $^{\circ}$ C. 103

Our group previously found a significant increase in the yield of F (up to 92 mol %) when PFOA or PFOS was heated at 700–900 °C. 65 The fast decomposition of PFAS and their volatile decomposition products at 890 °C may result in the high yield of F observed previously 65 and the fewer volatile thermal decomposition products detected in this study (Figure 6).

Conclusions. This paper presents a detailed investigation of the thermal degradation of PFAS in soil, focusing on the effect of temperature, thermal treatment time, initial contamination level, and soil texture. Several novel observations were made that are highly relevant to the thermal remediation of PFAS-contaminated soil. This study demonstrated that thermal treatment of soil at moderate temperatures is effective for decomposition of PFAS of various classes. Appropriate temperature (\geq 500 °C) and time (\geq 30 min) combinations led to a near-complete decomposition of the studied PFAS in either an air or a N₂ atmosphere. Performing pyrolysis on solid materials in an inert atmosphere may prevent the generation of dioxins and furans as observed in combustion/incineration processes. 104–107 The thermal stability followed the order: PFSAs > 6:2 Cl-PFAES \approx 8:2 FTS \approx PFCAs > N-MeFOSAA > HFPO-DA.

On the other hand, while thermal treatment holds promise for degradation of PFAS chemicals, the emission of volatile organofluorine species during thermal decomposition of PFAS may prove to be a significant challenge. This study indicates that various nonpolar products, particularly perfluoroalkenes, are generated from PFOA and PFOS at moderate temperatures (Figure 6), which require further treatment. Short-chain perfluoroalkanes of significant concern,60 such as perfluoromethane and perfluoroethane, were not observed. However, further studies are required to determine whether other PFAS under thermal conditions generate short-chain perfluoroalkanes that are greenhouse gases and more thermally stable 108 than PFAS. Last, handling of F radicals that may form corrosive hydrogen fluoride represents another technological challenge to thermally treat PFAS-containing materials.⁶⁰ The findings of this study demonstrated that the emission of F radicals can be significantly reduced with the presence of kaolinite or soil.

ASSOCIATED CONTENT

Supporting Information

The Supporting Information is available free of charge at https://pubs.acs.org/doi/10.1021/acsestengg.1c00335.

Adsorption experiment, thermal treatments of PFAS in soil, UPLC-QToF-MS/MS method, TD-Pyr-CT-GC-MS method, QA/QC, PFAS chemicals used in this study, 3M AFFF samples and cationic/zwitterionic PFAS used in this study, possible pyrolysis products of six PFAS chemicals identified in this study, experimental schematic diagram, recovery of PFCAs, PFSAs, and HFPO-DA from the soil, thermal decomposition of PFOA and PFOS in the soil in a tube furnace under a flow of N2 and in a sealed container with air, thermal decomposition of model cationic and zwitterionic PFAS in the soil, thermal decomposition of PFSAs and polyfluorinated compounds present in AFFF, effect of soil texture on the thermal decomposition of PFOA, effect of soil on the apparent yield of F from PFOA heated for 30 min at different temperatures, XRD and

FTIR spectra of kaolinite, PFOA, and PFOA-laden kaolinite particles after thermal treatments, possible formation pathways of perfluoroalkenes and perfluoroalkanes from PFAS during heating, and TD-Pyr-CT-GC-MS spectra of pyrolysis products of PFAS (PDF)

AUTHOR INFORMATION

Corresponding Author

Feng Xiao — Department of Civil Engineering, University of North Dakota, Grand Forks, North Dakota 58202, United States; orcid.org/0000-0001-5686-6055; Phone: +1-701-747-5150; Email: Feng.Xiao@UND.edu, fxiaoee@gmail.com; Fax: +1-701-777-3782

Authors

- Ali Alinezhad Department of Civil Engineering, University of North Dakota, Grand Forks, North Dakota 58202, United States
- Pavankumar Challa Sasi Department of Civil Engineering, University of North Dakota, Grand Forks, North Dakota 58202, United States
- Ping Zhang School of Resources Environmental and Chemical Engineering, Nanchang University, Nanchang 330031, PR China
- Bin Yao Department of Civil Engineering, University of North Dakota, Grand Forks, North Dakota 58202, United States; Department of Chemistry, University of North Dakota, Grand Forks, North Dakota 58202, United States
- Alena Kubátová Department of Chemistry, University of North Dakota, Grand Forks, North Dakota 58202, United States; ocid.org/0000-0002-2318-5883
- Svetlana A. Golovko Department of Biomedical Sciences, University of North Dakota, Grand Forks, North Dakota 58202, United States
- Mikhail Y. Golovko Department of Biomedical Sciences, University of North Dakota, Grand Forks, North Dakota 58202, United States

Complete contact information is available at: https://pubs.acs.org/10.1021/acsestengg.1c00335

Notes

The authors declare no competing financial interest.

■ ACKNOWLEDGMENTS

This work was mainly supported by the U.S. National Science Foundation CAREER Program (2047062; F.X.). Partial supports from the USEPA STAR Program (RD839660; F.X.) and the U.S. Department of Defense SERDP grant (ER21-1185; F.X.) are also gratefully acknowledged. The UPLC and the hybrid QToF-MS/MS systems, available in the Department of Biomedical Sciences at the University of North Dakota, were purchased under the NIH funded COBRE Mass Spec Core Facility Grant 5P30GM103329-05 (M.Y.G.). A.A. and P.C.S. were also supported by graduate fellowships supported by the US Geological Survey (FAR0032661 and FAR35039). B.Y. was supported by the University of North Dakota Pilot Postdoctoral Program from the Office of Vice President for Research & Economic Development. Finally, the authors gratefully acknowledge anonymous reviewers for their constructive comments toward improving the scientific quality of this paper. Any opinions, findings, and conclusions or recommendations expressed in this material are those of the author(s) and do not necessarily reflect the views of the NSF, EPA, and DoD.

REFERENCES

- (1) Paul, A. G.; Jones, K. C.; Sweetman, A. J. A first global production, emission, and environmental inventory for perfluor-octane sulfonate. *Environ. Sci. Technol.* **2009**, *43*, 386–392.
- (2) Prevedouros, K.; Cousins, I. T.; Buck, R. C.; Korzeniowski, S. H. Sources, fate and transport of perfluorocarboxylates. *Environ. Sci. Technol.* **2006**, *40*, 32–44.
- (3) Xiao, F. Emerging poly- and perfluoroalkyl substances in the aquatic environment: A review of current literature. *Water Res.* **2017**, 124, 482–495.
- (4) Wang, Z.; DeWitt, J. C.; Higgins, C. P.; Cousins, I. T. A neverending story of per- and polyfluoroalkyl substances (PFASs)? *Environ. Sci. Technol.* **2017**, *51*, 2508–2518.
- (5) Barzen-Hanson, K. A.; Roberts, S. C.; Choyke, S.; Oetjen, K.; McAlees, A.; Riddell, N.; McCrindle, R.; Ferguson, P. L.; Higgins, C. P.; Field, J. A. Discovery of 40 classes of per- and polyfluoroalkyl substances in historical aqueous film-forming foams (AFFFs) and AFFF-impacted groundwater. *Environ. Sci. Technol.* **2017**, *S1*, 2047–2057.
- (6) Strynar, M.; Dagnino, S.; McMahen, R.; Liang, S.; Lindstrom, A.; Andersen, E.; McMillan, L.; Thurman, M.; Ferrer, I.; Ball, C. Identification of novel perfluoroalkyl ether carboxylic acids (PFECAs) and sulfonic acids (PFESAs) in natural waters using accurate mass time-of-flight mass spectrometry (TOFMS). *Environ. Sci. Technol.* **2015**, 49, 11622–11630.
- (7) Wang, S.; Huang, J.; Yang, Y.; Hui, Y.; Ge, Y.; Larssen, T.; Yu, G.; Deng, S.; Wang, B.; Harman, C. First report of a Chinese PFOS alternative overlooked for 30 years: Its toxicity, persistence, and presence in the environment. *Environ. Sci. Technol.* **2013**, *47*, 10163–10170.
- (8) Ruan, T.; Lin, Y.; Wang, T.; Liu, R.; Jiang, G. Identification of novel polyfluorinated ether sulfonates as PFOS alternatives in municipal sewage sludge in China. *Environ. Sci. Technol.* **2015**, 49, 6519–6527.
- (9) Place, B. J.; Field, J. A. Identification of novel fluorochemicals in aqueous film-forming foams used by the US military. *Environ. Sci. Technol.* **2012**, *46*, 7120–7127.
- (10) D'Agostino, L. A.; Mabury, S. A. Identification of novel fluorinated surfactants in aqueous film forming foams and commercial surfactant concentrates. *Environ. Sci. Technol.* **2014**, *48*, 121–129.
- (11) Xiao, F.; Golovko, S. A.; Golovko, M. Y. Identification of novel non-ionic, cationic, zwitterionic, and anionic polyfluoroalkyl substances using UPLC-TOF-MS(E) high-resolution parent ion search. *Anal. Chim. Acta* **2017**, 988, 41–49.
- (12) Washington, J. W.; Rosal, C. G.; McCord, J. P.; Strynar, M. J.; Lindstrom, A. B.; Bergman, E. L.; Goodrow, S. M.; Tadesse, H. K.; Pilant, A. N.; Washington, B. J.; Davis, M. J.; Stuart, B. G.; Jenkins, T. M. Nontargeted mass-spectral detection of chloroperfluoropolyether carboxylates in New Jersey soils. *Science* **2020**, *368*, 1103–1107.
- (13) Barrett, H.; Du, X.; Houde, M.; Lair, S.; Verreault, J.; Peng, H. Suspect and nontarget screening revealed class-specific temporal trends (2000-2017) of poly- and perfluoroalkyl substances in St. Lawrence Beluga whales. *Environ. Sci. Technol.* **2021**, 55, 1659–1671.
- (14) Liu, Y.; D'Agostino, L. A.; Qu, G.; Jiang, G.; Martin, J. W. Highresolution mass spectrometry (HRMS) methods for nontarget discovery and characterization of poly- and per-fluoroalkyl substances (PFASs) in environmental and human samples. *TrAC, Trends Anal. Chem.* **2019**, *121*, 115420.
- (15) McDonough, C. A.; Choyke, S.; Barton, K. E.; Mass, S.; Starling, A. P.; Adgate, J. L.; Higgins, C. P. Unsaturated PFOS and other PFASs in human serum and drinking water from an AFFF-impacted community. *Environ. Sci. Technol.* **2021**, *55*, 8139–8148.
- (16) Yi, S.; Zhu, L.; Mabury, S. A. First report on in vivo pharmacokinetics and biotransformation of chlorinated polyfluoroalkyl ether sulfonates in rainbow trout. *Environ. Sci. Technol.* **2020**, *54*, 345–354.

- (17) Langberg, H. A.; Breedveld, G. D.; Slinde, G. A.; Grønning, H. M.; Høisæter, Å.; Jartun, M.; Rundberget, T.; Jenssen, B. M.; Hale, S. E. Fluorinated precursor compounds in sediments as a source of perfluorinated alkyl acids (PFAA) to biota. *Environ. Sci. Technol.* **2020**, *54*, 13077–13089.
- (18) Cui, Q.; Pan, Y.; Zhang, H.; Sheng, N.; Wang, J.; Guo, Y.; Dai, J. Occurrence and tissue distribution of novel perfluoroether carboxylic and sulfonic acids and legacy per/polyfluoroalkyl substances in black-spotted frog (Pelophylax nigromaculatus). *Environ. Sci. Technol.* **2018**, 52, 982–990.
- (19) Steenland, K.; Tinker, S.; Shankar, A.; Ducatman, A. Association of perfluorooctanoic acid (PFOA) and perfluorooctane sulfonate (PFOS) with uric acid among adults with elevated community exposure to PFOA. *Environ. Health Perspect.* **2010**, *118*, 229–233.
- (20) Melzer, D.; Rice, N.; Depledge, M. H.; Henley, W. E.; Galloway, T. S. Association between serum perfluorooctanoic acid (PFOA) and thyroid disease in the US national health and nutrition examination survey. *Environ. Health Perspect.* **2010**, *118*, 686–692.
- (21) Hoffman, K.; Webster, T. F.; Weisskopf, M. G.; Weinberg, J.; Vieira, V. M. Exposure to polyfluoroalkyl chemicals and attention deficit/hyperactivity disorder in U.S. children 12–15 years of age. *Environ. Health Perspect.* **2010**, *118*, 1762–1767.
- (22) Grandjean, P.; Budtz-Jørgensen, E. Immunotoxicity of perfluorinated alkylates: Calculation of benchmark doses based on serum concentrations in children. *Environ. Health* **2013**, *12*, 35.
- (23) USEPA. Announcement of final regulatory determinations for contaminants on the fourth drinking water contaminant candidate list. *Fed. Regist.* **2021**, *86*, 12272–12291.
- (24) Takagi, S.; Adachi, F.; Miyano, K.; Koizumi, Y.; Tanaka, H.; Watanabe, I.; Tanabe, S.; Kannan, K. Fate of Perfluorooctanesulfonate and perfluorooctanoate in drinking water treatment processes. *Water Res.* 2011, 45, 3925–3932.
- (25) Eschauzier, C.; Beerendonk, E.; Scholte-Veenendaal, P.; de Voogt, P. Impact of treatment processes on the removal of perfluoroalkyl acids from the drinking water production chain. *Environ. Sci. Technol.* **2012**, *46*, 1708–1715.
- (26) Mejia Avendaño, S.; Zhong, G.; Liu, J. Comment on "Biodegradation of perfluorooctanesulfonate (PFOS) as an emerging contaminant". *Chemosphere* **2015**, *138*, 1037–1038.
- (27) Yu, J.; Hu, J.; Tanaka, S.; Fujii, S. Perfluorooctane sulfonate (PFOS) and perfluorooctanoic acid (PFOA) in sewage treatment plants. *Water Res.* **2009**, *43*, 2399–2408.
- (28) Xiao, F.; Halbach, T. R.; Simcik, M. F.; Gulliver, J. S. Input characterization of perfluoroalkyl substances in wastewater treatment plants: Source discrimination by exploratory data analysis. *Water Res.* **2012**, *46*, 3101–3109.
- (29) Xiao, F.; Simcik, M. F.; Gulliver, J. S. Mechanisms for removal of perfluorooctane sulfonate (PFOS) and perfluorooctanoate (PFOA) from drinking water by conventional and enhanced coagulation. *Water Res.* **2013**, *47*, *49*–56.
- (30) PFAS in the revised drinking water directive (DWD). https://www.eurofins.se/tjaenster/miljoe-och-vatten/nyheter-miljo/pfas-in-the-revised-drinking-water-directive-dwd/ (accessed November 2021).
- (31) Hale, S. E.; Arp, H. P. H.; Schliebner, I.; Neumann, M. Persistent, mobile and toxic (PMT) and very persistent and very mobile (vPvM) substances pose an equivalent level of concern to persistent, bioaccumulative and toxic (PBT) and very persistent and very bioaccumulative (vPvB) substances under REACH. *Environ. Sci. Eur.* 2020, 32, 155.
- (32) Xiao, F.; Simcik, M. F.; Halbach, T. R.; Gulliver, J. S. Perfluorooctane sulfonate (PFOS) and perfluorooctanoate (PFOA) in soils and groundwater of a U.S. metropolitan area: Migration and implications for human exposure. *Water Res.* 2015, 72, 64–74.
- (33) Stahl, T.; Heyn, J.; Thiele, H.; Hüther, J.; Failing, K.; Georgii, S.; Brunn, H. Carryover of perfluorooctanoic acid (PFOA) and perfluorooctane sulfonate (PFOS) from soil to plants. *Arch. Environ. Contam. Toxicol.* **2009**, *57*, 289–298.

- (34) Lechner, M.; Knapp, H. Carryover of perfluorooctanoic acid (PFOA) and perfluorooctane sulfonate (PFOS) from soil to plant and distribution to the different plant compartments studied in cultures of carrots (*Daucus carota ssp Sativus*), potatoes (*Solanum tuberosum*), and cucumbers (*Cucumis Sativus*). *J. Agric. Food Chem.* **2011**, *59*, 11011–11018.
- (35) Moody, C. A.; Field, J. A. Determination of perfluorocarboxylates in groundwater impacted by fire-fighting activity. *Environ. Sci. Technol.* **1999**, 33, 2800–2806.
- (36) Houtz, E. F.; Higgins, C. P.; Field, J. A.; Sedlak, D. L. Persistence of perfluoroalkyl acid precursors in AFFF-impacted groundwater and soil. *Environ. Sci. Technol.* **2013**, *47*, 8187–8195.
- (37) Backe, W. J.; Day, T. C.; Field, J. A. Zwitterionic, cationic, and anionic fluorinated chemicals in aqueous film forming foam formulations and groundwater from U.S. military bases by non-aqueous large-volume injection HPLC-MS/MS. *Environ. Sci. Technol.* **2013**. 47, 5226–5234.
- (38) Høisæter, Å.; Pfaff, A.; Breedveld, G. D. Leaching and transport of PFAS from aqueous film-forming foam (AFFF) in the unsaturated soil at a firefighting training facility under cold climatic conditions. *J. Contam. Hydrol.* **2019**, 222, 112–122.
- (39) Filipovic, M.; Woldegiorgis, A.; Norström, K.; Bibi, M.; Lindberg, M.; Österås, A.-H. Historical usage of aqueous film forming foam: A case study of the widespread distribution of perfluoroalkyl acids from a military airport to groundwater, lakes, soils and fish. *Chemosphere* **2015**, *129*, 39–45.
- (40) Davis, K. L.; Aucoin, M. D.; Larsen, B. S.; Kaiser, M. A.; Hartten, A. S. Transport of ammonium perfluorooctanoate in environmental media near a fluoropolymer manufacturing facility. *Chemosphere* **2007**, *67*, 2011–2019.
- (41) Emmett, E. A.; Shofer, F. S.; Zhang, H.; Freeman, D.; Desai, C.; Shaw, L. M. Community exposure to perfluorooctanoate: Relationships between serum concentrations and exposure sources. *J. Occup. Environ. Med.* **2006**, *48*, 759–770.
- (42) Hoffman, K.; Webster, T. F.; Bartell, S. M.; Weisskopf, M. G.; Fletcher, T.; Vieira, V. M. Private drinking water wells as a source of exposure to perfluorooctanoic acid (PFOA) in communities surrounding a fluoropolymer production facility. *Environ. Health Perspect.* **2011**, *119*, 92–97.
- (43) Lang, J. R.; Allred, B. M.; Peaslee, G. F.; Field, J. A.; Barlaz, M. A. Release of per- and polyfluoroalkyl substances (PFASs) from carpet and clothing in model anaerobic landfill reactors. *Environ. Sci. Technol.* **2016**, *50*, 5024–5032.
- (44) Li, B.; Danon-Schaffer, M. N.; Li, L. Y.; Ikonomou, M. G.; Grace, J. R. Occurrence of PFCs and PBDEs in landfill leachates from across Canada. *Water, Air, Soil Pollut.* **2012**, 223, 3365–3372.
- (45) Yoo, H.; Washington, J. W.; Ellington, J. J.; Jenkins, T. M.; Neill, M. P. Concentrations, distribution, and persistence of fluorotelomer alcohols in sludge-applied soils near Decatur, Alabama, USA. *Environ. Sci. Technol.* **2010**, *44*, 8397–8402.
- (46) Washington, J. W.; Yoo, H.; Ellington, J. J.; Jenkins, T. M.; Libelo, E. L. Concentrations, distribution, and persistence of perfluoroalkylates in sludge-applied soils near Decatur, Alabama, USA. *Environ. Sci. Technol.* **2010**, *44*, 8390–8396.
- (47) Plumlee, M. H.; Larabee, J.; Reinhard, M. Perfluorochemicals in water reuse. *Chemosphere* **2008**, *72*, 1541–1547.
- (48) DOD. Aqueous Film Forming Foam Report to Congress, 2017.
- (49) Senevirathna, S. T. M. L. D.; Mahinroosta, R.; Li, M.; KrishnaPillai, K. In situ soil flushing to remediate confined soil contaminated with PFOS- an innovative solution for emerging environmental issue. *Chemosphere* **2021**, 262, 127606.
- (50) Bentel, M. J.; Liu, Z.; Yu, Y.; Gao, J.; Men, Y.; Liu, J. Enhanced degradation of perfluorocarboxylic acids (PFCAs) by UV/sulfite treatment: Reaction mechanisms and system efficiencies at pH 12. *Environ. Sci. Technol. Lett.* **2020**, *7*, 351–357.
- (51) Qanbarzadeh, M.; Wang, D.; Ateia, M.; Sahu, S. P.; Cates, E. L. Impacts of reactor configuration, degradation mechanisms, and water matrices on perfluorocarboxylic acid treatment efficiency by the UV/

- $Bi_3O(OH)(PO_4)_2$ photocatalytic process. ACS ES&T Engg 2021, 1, 239–248.
- (52) Tenorio, R.; Liu, J.; Xiao, X.; Maizel, A.; Higgins, C. P.; Schaefer, C. E.; Strathmann, T. J. Destruction of per- and polyfluoroalkyl substances (PFASs) in aqueous film-forming foam (AFFF) with UV-sulfite photoreductive treatment. *Environ. Sci. Technol.* **2020**, *54*, 6957–6967.
- (53) Hale, S. E.; Arp, H. P. H.; Slinde, G. A.; Wade, E. J.; Bjørseth, K.; Breedveld, G. D.; Straith, B. F.; Moe, K. G.; Jartun, M.; Høisæter, Å. Sorbent amendment as a remediation strategy to reduce PFAS mobility and leaching in a contaminated sandy soil from a Norwegian firefighting training facility. *Chemosphere* **2017**, *171*, 9–18.
- (54) Sørmo, E.; Silvani, L.; Bjerkli, N.; Hagemann, N.; Zimmerman, A. R.; Hale, S. E.; Hansen, C. B.; Hartnik, T.; Cornelissen, G. Stabilization of PFAS-contaminated soil with activated biochar. *Sci. Total Environ.* **2021**, 763, 144034.
- (55) Turner, L. P.; Kueper, B. H.; Jaansalu, K. M.; Patch, D. J.; Battye, N.; El-Sharnouby, O.; Mumford, K. G.; Weber, K. P. Mechanochemical remediation of perfluorooctanesulfonic acid (PFOS) and perfluorooctanoic acid (PFOA) amended sand and aqueous film-forming foam (AFFF) impacted soil by planetary ball milling. Sci. Total Environ. 2021, 765, 142722.
- (56) Schaefer, C. E.; Choyke, S.; Ferguson, P. L.; Andaya, C.; Burant, A.; Maizel, A.; Strathmann, T. J.; Higgins, C. P. Electrochemical transformations of perfluoroalkyl acid (PFAA) precursors and PFAAs in groundwater impacted with aqueous film forming foams. *Environ. Sci. Technol.* **2018**, *52*, 10689–10697.
- (57) Le, T. X. H.; Haflich, H.; Shah, A. D.; Chaplin, B. P. Energy-efficient electrochemical oxidation of perfluoroalkyl substances using a Ti4O7 reactive electrochemical membrane anode. *Environ. Sci. Technol. Lett.* **2019**, *6*, 504–510.
- (58) Wu, B.; Hao, S.; Choi, Y.; Higgins, C. P.; Deeb, R.; Strathmann, T. J. Rapid destruction and defluorination of perfluorooctanesulfonate by alkaline hydrothermal reaction. *Environ. Sci. Technol. Lett.* **2019**, *6*, 630–636.
- (59) Hao, S.; Choi, Y.-J.; Wu, B.; Higgins, C. P.; Deeb, R.; Strathmann, T. J. Hydrothermal alkaline treatment for destruction of per- and polyfluoroalkyl substances in aqueous film-forming foam. *Environ. Sci. Technol.* **2021**, *55*, 3283–3295.
- (60) USEPA. Interim Guidance on the Destruction and Disposal of Perfluoroalkyl and Polyfluoroalkyl Substances and Materials Containing Perfluoroalkyl and Polyfluoroalkyl Substances, 2020.
- (61) Crownover, E.; Oberle, D.; Kluger, M.; Heron, G. Perfluoroalkyl and polyfluoroalkyl substances thermal desorption evaluation. *Remediation* **2019**, *29*, 77–81.
- (62) Duchesne, A. L.; Brown, J. K.; Patch, D. J.; Major, D.; Weber, K. P.; Gerhard, J. I. Remediation of PFAS-contaminated soil and granular activated carbon by smoldering combustion. *Environ. Sci. Technol.* **2020**, *54*, 12631–12640.
- (63) Watanabe, N.; Takata, M.; Takemine, S.; Yamamoto, K. Thermal mineralization behavior of PFOA, PFHxA, and PFOS during reactivation of granular activated carbon (GAC) in nitrogen atmosphere. *Environ. Sci. Pollut. Res. Int.* **2018**, *25*, 7200–7205.
- (64) Sasi, P. C.; Alinezhad, A.; Yao, B.; Kubátová, A.; Golovko, S. A.; Golovko, M. Y.; Xiao, F. Effect of granular activated carbon and other porous materials on thermal decomposition of per- and polyfluor-oalkyl substances: Mechanisms and implications for water purification. *Water Res.* **2021**, *200*, 117271.
- (65) Xiao, F.; Sasi, P. C.; Yao, B.; Kubátová, A.; Golovko, S. A.; Golovko, M. Y.; Soli, D. Thermal stability and decomposition of perfluoroalkyl substances on spent granular activated carbon. *Environ. Sci. Technol. Lett.* **2020**, *7*, 343–350.
- (66) Wang, F.; Shih, K.; Lu, X.; Liu, C. Mineralization behavior of fluorine in perfluorooctanesulfonate (PFOS) during thermal treatment of lime-conditioned sludge. *Environ. Sci. Technol.* **2013**, 47, 2621–2627.
- (67) Xiao, F.; Sasi, P. C.; Alinezhad, A.; Golovko, S. A.; Golovko, M. Y.; Spoto, A. Thermal decomposition of anionic, zwitterionic, and

- cationic polyfluoroalkyl substances in aqueous film-forming foams. *Environ. Sci. Technol.* **2021**, *55*, 9885–9894.
- (68) Xiao, F.; Sasi, P. C.; Yao, B.; Kubátová, A.; Golovko, S. A.; Golovko, M. Y.; Soli, D. Thermal Decomposition of PFAS: Response to Comment on "Thermal Stability and Decomposition of Perfluoroalkyl Substances on Spent Granular Activated Carbon". *Environ. Sci. Technol. Lett.* **2021**, *8*, 364–365.
- (69) Krusic, P. J.; Roe, D. C. Gas-phase NMR technique for studying the thermolysis of materials: Thermal decomposition of ammonium perfluorooctanoate. *Anal. Chem.* **2004**, *76*, 3800–3803.
- (70) EPA. Risk Management for Per- and Polyfluoroalkyl Substances (PFASs) under TSCA. https://www.epa.gov/assessing-and-managing-chemicals-under-tsca/risk-management-and-polyfluoroalkyl-substances-pfas (accessed June 2017).
- (71) Wang, T.; Wang, Y.; Liao, C.; Cai, Y.; Jiang, G. Perspectives on the inclusion of perfluorooctane sulfonate into the Stockholm Convention on persistent organic pollutants. *Environ. Sci. Technol.* **2009**, 43, 5171–5175.
- (72) Wang, Z.; Cousins, I. T.; Scheringer, M.; Hungerbühler, K. Fluorinated alternatives to long-chain perfluoroalkyl carboxylic acids (PFCAs), perfluoroalkane sulfonic acids (PFSAs) and their potential precursors. *Environ. Int.* **2013**, *60*, 242–248.
- (73) Heydebreck, F.; Tang, J.; Xie, Z.; Ebinghaus, R. Alternative and legacy perfluoroalkyl substances: Differences between European and Chinese river/estuary systems. *Environ. Sci. Technol.* **2015**, *49*, 8386–8395
- (74) Sun, M.; Arevalo, E.; Strynar, M.; Lindstrom, A.; Richardson, M.; Kearns, B.; Pickett, A.; Smith, C.; Knappe, D. R. U. Legacy and emerging perfluoroalkyl substances are important drinking water contaminants in the Cape Fear River watershed of North Carolina. *Environ. Sci. Technol. Lett.* **2016**, *3*, 415–419.
- (75) Gebbink, W. A.; van Leeuwen, S. P. J. Environmental contamination and human exposure to PFASs near a fluorochemical production plant: Review of historic and current PFOA and GenX contamination in the Netherlands. *Environ. Int.* **2020**, *137*, 105583.
- (76) Li, J.; He, J.; Niu, Z.; Zhang, Y. Legacy per- and polyfluoroalkyl substances (PFASs) and alternatives (short-chain analogues, F-53B, GenX and FC-98) in residential soils of China: Present implications of replacing legacy PFASs. *Environ. Int.* **2020**, *135*, 105419.
- (77) Xiao, F.; Hanson, R. A.; Golovko, S. A.; Golovko, M. Y.; Arnold, W. A. PFOA and PFOS are generated from zwitterionic and cationic precursor compounds during water disinfection with chlorine or ozone. *Environ. Sci. Technol. Lett.* **2018**, *5*, 382–388.
- (78) Jin, B.; Mallula, S.; Golovko, S. A.; Golovko, M. Y.; Xiao, F. In vivo generation of PFOA, PFOS, and other compounds from cationic and zwitterionic per- and polyfluoroalkyl substances in a terrestrial invertebrate (Lumbricus terrestris). *Environ. Sci. Technol.* **2020**, *54*, 7378–7387.
- (79) Nickerson, A.; Rodowa, A. E.; Adamson, D. T.; Field, J. A.; Kulkarni, P. R.; Kornuc, J. J.; Higgins, C. P. Spatial trends of anionic, zwitterionic, and cationic PFASs at an AFFF-Impacted site. *Environ. Sci. Technol.* **2021**, *55*, 313–323.
- (80) Xiao, F.; Jin, B.; Golovko, S. A.; Golovko, M. Y.; Xing, B. Sorption and desorption mechanisms of cationic and zwitterionic perand polyfluoroalkyl substances in natural soils: Thermodynamics and hysteresis. *Environ. Sci. Technol.* **2019**, *53*, 11818–11827.
- (81) Xiao, F.; Zhang, X.; Penn, L.; Gulliver, J. S.; Simcik, M. F. Effects of monovalent cations on the competitive adsorption of perfluoroalkyl acids by kaolinite: Experimental studies and modeling. *Environ. Sci. Technol.* **2011**, *45*, 10028–10035.
- (82) Xiao, F.; Gámiz, B.; Pignatello, J. J. Adsorption and desorption of nitrous oxide by raw and thermally air-oxidized chars. *Sci. Total Environ.* **2018**, *643*, 1436–1445.
- (83) Vidonish, J. E.; Zygourakis, K.; Masiello, C. A.; Sabadell, G.; Alvarez, P. J. J. Thermal treatment of hydrocarbon-impacted soils: A review of technology innovation for sustainable remediation. *Engineering* **2016**, *2*, 426–437.
- (84) Higgins, C. P.; Luthy, R. G. Sorption of perfluorinated surfactants on sediments. *Environ. Sci. Technol.* **2006**, 40, 7251–7256.

- (85) Du, Z.; Deng, S.; Bei, Y.; Huang, Q.; Wang, B.; Huang, J.; Yu, G. Adsorption behavior and mechanism of perfluorinated compounds on various adsorbents-a review. *J. Hazard. Mater.* **2014**, 274, 443–454.
- (86) Wang, F.; Shih, K. Adsorption of perfluorooctanesulfonate (PFOS) and perfluorooctanoate (PFOA) on alumina: Influence of solution pH and cations. *Water Res.* **2011**, *45*, 2925–2930.
- (87) Ferrey, M. L.; Wilson, J. T.; Adair, C.; Su, C.; Fine, D. D.; Liu, X.; Washington, J. W. Behavior and fate of PFOA and PFOS in sandy aquifer sediment. *Ground Water Monit. Rev.* **2012**, 32, 63–71.
- (88) Milinovic, J.; Lacorte, S.; Vidal, M.; Rigol, A. Sorption behaviour of perfluoroalkyl substances in soils. *Sci. Total Environ.* **2015**, *511*, 63–71.
- (89) Xiao, F.; Davidsavor, K. J.; Park, S.; Nakayama, M.; Phillips, B. R. Batch and column study: Sorption of perfluorinated surfactants from water and cosolvent systems by Amberlite XAD resins. *J. Colloid Interface Sci.* **2012**, 368, 505–511.
- (90) Chen, H.; Reinhard, M.; Nguyen, V. T.; Gin, K. Y.-H. Reversible and irreversible sorption of perfluorinated compounds (PFCs) by sediments of an urban reservoir. *Chemosphere* **2016**, *144*, 1747–1753.
- (91) Weston, J. S.; Harwell, J. H.; Shiau, B. J.; Kabir, M. Disrupting admicelle formation and preventing surfactant adsorption on metal oxide surfaces using sacrificial polyelectrolytes. *Langmuir* **2014**, *30*, 6384–6388.
- (92) Nayyar, S. P.; Sabatini, D. A.; Harwell, J. H. Surfactant adsolubilization and modified admicellar sorption of nonpolar, polar, and ionizable organic contaminants. *Environ. Sci. Technol.* **1994**, 28, 1874–1881.
- (93) Adak, A.; Bandyopadhyay, M.; Pal, A. Adsorption of anionic surfactant on alumina and reuse of the surfactant-modified alumina for the removal of crystal violet from aquatic environment. *J. Environ. Sci. Health, Part A: Toxic/Hazard. Subst. Environ. Eng.* **2005**, 40, 167–182.
- (94) Zhang, R.; Somasundaran, P. Advances in adsorption of surfactants and their mixtures at solid/solution interfaces. *Adv. Colloid Interface Sci.* **2006**, 123–126, 213–229.
- (95) Johnson, R. L.; Anschutz, A. J.; Smolen, J. M.; Simcik, M. F.; Penn, R. L. The adsorption of perfluorooctane sulfonate onto sand, clay, and iron oxide surfaces. *J. Chem. Eng. Data* **2007**, *52*, 1165–1170.
- (96) Mulder, I.; Schmittdiel, M.; Frei, H.; Hofmann, L.; Gerbig, D.; Siemens, J. Soil water solutes reduce the critical micelle concentration of quaternary ammonium compounds. *Environ. Sci. Pollut. Res. Int.* **2020**, *27*, 45311–45323.
- (97) Campos Pereira, H.; Ullberg, M.; Kleja, D. B.; Gustafsson, J. P.; Ahrens, L. Sorption of perfluoroalkyl substances (PFASs) to an organic soil horizon Effect of cation composition and pH. *Chemosphere* **2018**, 207, 183–191.
- (98) Bentel, M. J.; Yu, Y.; Xu, L.; Kwon, H.; Li, Z.; Wong, B. M.; Men, Y.; Liu, J. Degradation of perfluoroalkyl ether carboxylic acids with hydrated electrons: Structure-reactivity relationships and environmental implications. *Environ. Sci. Technol.* **2020**, *54*, 2489–2499.
- (99) Kontozova-Deutsch, V.; Deutsch, F.; Bencs, L.; Krata, A.; Van Grieken, R.; De Wael, K. Optimization of the ion chromatographic quantification of airborne fluoride, acetate and formate in the Metropolitan Museum of Art, New York. *Talanta* 2011, 86, 372–376.
- (100) Rice, E. W.; Baird, R. B.; Eaton, A. D.; Clesceri, L. S. Standard Methods for the Examination of Water and Wastewater, 22nd ed.; American Public Health Association: Washington, D.C., 2012.
- (101) Semmens, B.; Meggy, A. B. The reaction of kaolin with fluorides: I. Effect of neutral and acid sodium fluoride solutions. *J. Appl. Chem.* **1966**, *16*, 122–125.
- (102) Winchell, L. J.; Ross, J. J.; Wells, M. J. M.; Fonoll, X.; Norton, J. W.; Bell, K. Y. Per- and polyfluoroalkyl substances thermal destruction at water resource recovery facilities: A state of the science review. *Water Environ. Res.* **2021**, *93*, 826–843.

- (103) Khan, M. Y.; So, S.; da Silva, G. Decomposition kinetics of perfluorinated sulfonic acids. *Chemosphere* **2020**, 238, 124615.
- (104) Hutzinger, O.; Choudhry, G. G.; Chittim, B. G.; Johnston, L. E. Formation of polychlorinated dibenzofurans and dioxins during combustion, electrical equipment fires and PCB incineration. *Environ. Health Perspect.* 1985, 60, 3–9.
- (105) Dyke, P. H.; Foan, C.; Fiedler, H. PCB and PAH releases from power stations and waste incineration processes in the UK. *Chemosphere* **2003**, *50*, 469–480.
- (106) Dopico, M.; Gómez, A. Review of the current state and main sources of dioxins around the world. *J. Air Waste Manage. Assoc.* **2015**, 65, 1033–1049.
- (107) Söderström, G.; Marklund, S. PBCDD and PBCDF from incineration of waste-containing brominated flame retardants. *Environ. Sci. Technol.* **2002**, *36*, 1959–1964.
- (108) Rogers, G. C.; Cady, G. H. Pyrolysis of perfluoro-*n*-pentane. *J. Am. Chem. Soc.* **1951**, *73*, 3523–3524.

